جامعة الانبار

كلية العلوم -قسم الجيولوجيا التطبيقية

اسم المادة بالعربي: الجيوفيزياء الجهدية - الطريقة المغناطيسية

اسم المادة بالإنكليزي: Potential Geophysics- Magnetic Method

عنوان المحاضرة: Reduction of magnetic observations

اسم المحاضر: الاستاذ الدكتور علي مشعل عبد حمد الحلبوسي

Reduction of magnetic observations

Reduction of magnetic observations

The reduction of magnetic data is necessary to remove all causes of magnetic variation from the observations other than those arising from the magnetic effects of the subsurface.

Diurnal variation correction

The effects of diurnal variation may be removed in several ways. On land a method similar to gravimeter drift monitoring may be employed in which the magnetometer is read at a fixed base station periodically throughout the day. The differences observed in base readings are then distributed among the readings at stations occupied during the day according to the time of observation. It should be remembered that base readings taken during a gravity survey are made to correct for both the drift of the gravimeter and tidal effects; magnetometers do not drift and base readings are taken solely to correct for temporal variation in the measured field. Such a procedure is inefficient as the instrument has to be returned periodically to a base location and is not practical in marine or airborne surveys. These problems may be overcome by use of a base magnetometer, a continuous-reading instrument which records magnetic variations at a fixed location within or close to the survey area. This method is preferable on land as the survey proceeds faster and the diurnal variations are fully charted. Where the survey is of regional extent the records of a magnetic observatory may be used. Such observatories continuously record changes in all the geomagnetic elements. However, diurnal variations differ quite markedly from place to place and so the observatory used should not be more than about 100 km from the survey area.

Diurnal variation during an aeromagnetic survey may alternatively be assessed by arranging numerous crossover points in the survey plan (Fig. 7.12). Analysis of the differences in readings at each crossover, representing the field change over a series of different time periods, allows the whole survey to be corrected for diurnal variation by a process of network adjustment, without the necessity of a base instrument.

Diurnal variations, however recorded, must be examined carefully. If large, high-frequency variations are apparent, resulting from a magnetic storm, the survey results should be discarded.

7.9.2 Geomagnetic correction

The magnetic equivalent of the latitude correction in gravity surveying is the *geomagnetic correction* which removes the effect of a geomagnetic reference field from the survey data. The most rigorous method of geomagnetic correction is the use of the IGRF (Section 7.4), which expresses the undisturbed geomagnetic field in terms of a large number of harmonics and includes temporal terms to correct for secular variation. The complexity of the IGRF requires the calculation of corrections by computer. It must be realized, however, that the IGRF is imperfect as the harmonics employed are based on observations at relatively few, scattered, magnetic observatories. The IGRF is also predictive in that it extrapolates forwards the spherical harmonics derived from observatory data. Consequently, the IGRF in areas remote from observatories can be substantially in error.

Over the area of a magnetic survey the geomagnetic reference field may be approximated by a uniform gradient defined in terms of latitudinal and longitudinal gradient components. For example, the geomagnetic field over the British Isles is approximated by the following gradient components: $2.13\,\mathrm{nT\,km^{-1}}$ N; $0.26\,\mathrm{nT\,km^{-1}}$ W; these vary with time. For any survey area the relevant gradient values may be assessed from magnetic maps covering a much larger region.

The appropriate regional gradients may also be obtained by employing a single dipole approximation of the Earth's field and using the well-known equations for the magnetic field of a dipole to derive local field gradients:

$$Z = \frac{\mu_0}{4\pi}\frac{2M}{R^3}\cos\theta, \qquad H = \frac{\mu_0}{4\pi}\frac{M}{R^3}\sin\theta \tag{7.12}$$

$$\frac{\partial Z}{\partial \theta} = -2H, \qquad \frac{\partial H}{\partial \theta} = \frac{Z}{2} \tag{7.13}$$

where Z and H are the vertical and horizontal field components, θ the colatitude in radians, R the radius of the Earth, M the magnetic moment of the Earth and $\partial Z/\partial\theta$ and $\partial H/\partial\theta$ the rate of change of Z and H with colatitude, respectively.

An alternative method of removing the regional gradient over a relatively small survey area is by use of trend analysis. A trend line (for profile data) or trend surface (for areal data) is fitted to the observations using the least squares criterion, and subsequently subtracted from the observed data to leave the local anomalies as positive and negative residuals (Fig. 7.13).

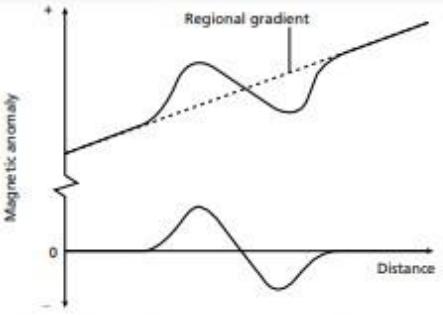

Fig. 7.13 The removal of a regional gradient from a magnetic field by trend analysis. The regional field is approximated by a linear trend.

7.9.3 Elevation and terrain corrections

The vertical gradient of the geomagnetic field is only some $0.03\,\mathrm{nT\,m^{-1}}$ at the poles and $-0.015\,\mathrm{nT\,m^{-1}}$ at the equator, so an *elevation correction* is not usually applied. The influence of topography can be significant in ground magnetic surveys but is not completely predictable as it depends upon the magnetic properties of the topographic features. Therefore, in magnetic surveying *terrain corrections* are rarely applied.

Having applied diurnal and geomagnetic corrections, all remaining magnetic field variations should be caused solely by spatial variations in the magnetic properties of the subsurface and are referred to as magnetic anomalies.

7.10 Interpretation of magnetic anomalies

7.10.1 Introduction

The interpretation of magnetic anomalies is similar in its procedures and limitations to gravity interpretation as both techniques utilize natural potential fields based on inverse square laws of attraction. There are several differences, however, which increase the complexity of magnetic interpretation.

Whereas the gravity anomaly of a causative body is entirely positive or negative, depending on whether the body is more or less dense than its surroundings, the magnetic anomaly of a finite body invariably contains positive and negative elements arising from the dipolar nature of magnetism (Fig. 7.14). Moreover, whereas

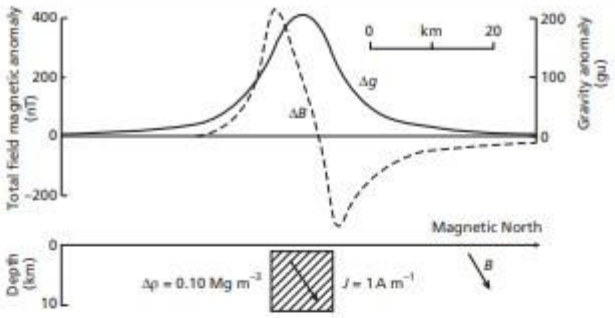

Fig. 7.14 Gravity (Δg) and magnetic (ΔB) anomalies over the same two-dimensional body.

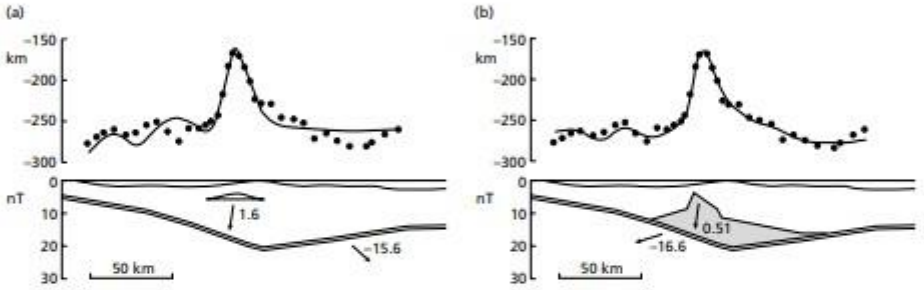

Fig. 7.15 An example of ambiguity in magnetic interpretation. The arrows correspond to the directions of magnetization vectors, whose magnitude is given in A m^{-1}. (After Westbrook 1975.)

density is a scalar, intensity of magnetization is a vector, and the direction of magnetization in a body closely controls the shape of its magnetic anomaly. Thus bodies of identical shape can give rise to very different magnetic anomalies. For the above reasons magnetic anomalies are often much less closely related to the shape of the causative body than are gravity anomalies.

The intensity of magnetization of a rock is largely dependent upon the amount, size, shape and distribution of its contained ferrimagnetic minerals and these represent only a small proportion of its constituents. By contrast, density is a bulk property. Intensity of magnetization can vary by a factor of 10^6 between different rock types, and is thus considerably more variable than density, where the range is commonly 1.50–3.50 Mg m^{-3}.

Magnetic anomalies are independent of the distance units employed. For example, the same magnitude anomaly is produced by, say, a 3 m cube (on a metre scale) as a 3 km cube (on a kilometre scale) with the same magnetic properties. The same is not true of gravity anomalies.

The problem of ambiguity in magnetic interpretation is the same as for gravity, that is, the same inverse problem is encountered. Thus, just as with gravity, all external controls on the nature and form of the causative body must be employed to reduce the ambiguity. An example of this problem is illustrated in Fig. 7.15, which shows two possible interpretations of a magnetic profile across the Barbados Ridge in the eastern Caribbean. In both cases the regional variations are attributed to the variation in depth of a 1 km thick oceanic crustal layer 2. The high-amplitude central anomaly, however, can be explained by either the presence of a detached sliver of oceanic crust (Fig. 7.15(a)) or a rise of metamorphosed sediments at depth (Fig. 7.15(b)).

Much qualitative information may be derived from a magnetic contour map. This applies especially to aeromagnetic maps which often provide major clues as to the

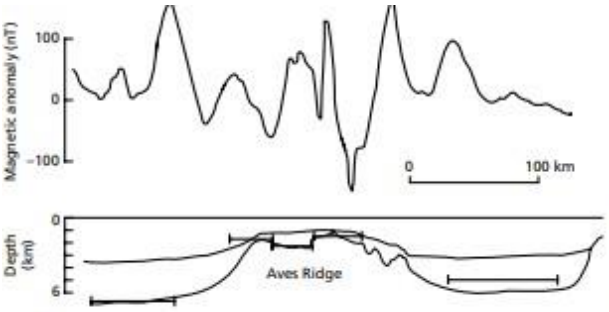

Fig. 7.16 Magnetic anomalies over the Aves Ridge, eastern Caribbean. Lower diagram illustrates bathymetry and basement/sediment interface. Horizontal bars indicate depth estimates of the magnetic basement derived by spectral analysis of the magnetic data.

geology and structure of a broad region from an assessment of the shapes and trends of anomalies. Sediment-covered areas with relatively deep basement are typically represented by smooth magnetic contours reflecting basement structures and magnetization contrasts. Igneous and metamorphic terrains generate far more complex magnetic anomalies, and the effects of deep geological features may be obscured by short-wavelength anomalies of near-surface origin. In most types of terrain an aeromagnetic map can be a useful aid to reconnaissance geological mapping. Such qualitative interpretations may be greatly facilitated by the use of digital image processing techniques (see Section 6.8.6).

In carrying out quantitative interpretation of magnetic anomalies, both direct and indirect methods may be employed, but the former are much more limited than for gravity interpretation and no equivalent general equations exist for total field anomalies.

7.10.2 Direct interpretation

Limiting depth is the most important parameter derived by direct interpretation, and this may be deduced from magnetic anomalies by making use of their property of decaying rapidly with distance from source. Magnetic anomalies caused by shallow structures are more dominated by short-wavelength components than those resulting from deeper sources. This effect may be quantified by computing the power spectrum of the anomaly as it can be shown, for certain types of source body, that the log-power spectrum has a linear gradient whose magnitude is dependent upon the depth of the source (Spector & Grant 1970). Such techniques of spectral analysis provide rapid depth estimates from regularly-spaced digital field data; no geomagnetic or diurnal corrections are necessary as these remove only low-wavenumber components and do not affect the depth estimates which are controlled by the high-wavenumber components of the observed field. Figure 7.16 shows a magnetic profile across the Aves Ridge in the eastern Caribbean. In this region the configuration of the sediment/basement interface is reasonably well known from both seismic reflection and refraction surveys. The magnetic anomalies clearly show their shortest wavelength over areas of relatively shallow basement, and this observation is quantified by the power spectral depth estimates (horizontal bars) which show excellent correlation with the known basement relief.

A more complex, but more rigorous method of determining the depth to magnetic sources derives from a technique known as *Euler deconvolution* (Reid *et al.* 1990). Euler's homogeneity relation can be written:

$$(x-x_0)\frac{\partial T}{\partial x}+(y-y_0)\frac{\partial T}{\partial y}+(z-z_0)\frac{\partial T}{\partial z}=N(B-T) \tag{7.14}$$

where (x_0, y_0, z_0) is the location of a magnetic source, whose total field magnetic anomaly at the point (x, y, z) is T and B is the regional field. N is a measure of the rate of change of a field with distance and assumes different values for different types of magnetic source. Equation (7.14) is solved by calculating or measuring the anomaly gradients for various areas of the anomaly and selecting a value for N. This method produces more rigorous depth estimates than other methods, but is considerably more difficult to implement. An example of an Euler deconvolution is shown in Fig. 7.17. The aeromagnetic field shown in Fig. 7.17(a) has the solutions shown in Fig. 17(b–d) for structural indices (N) of 0.0, 0.5 and 0.6

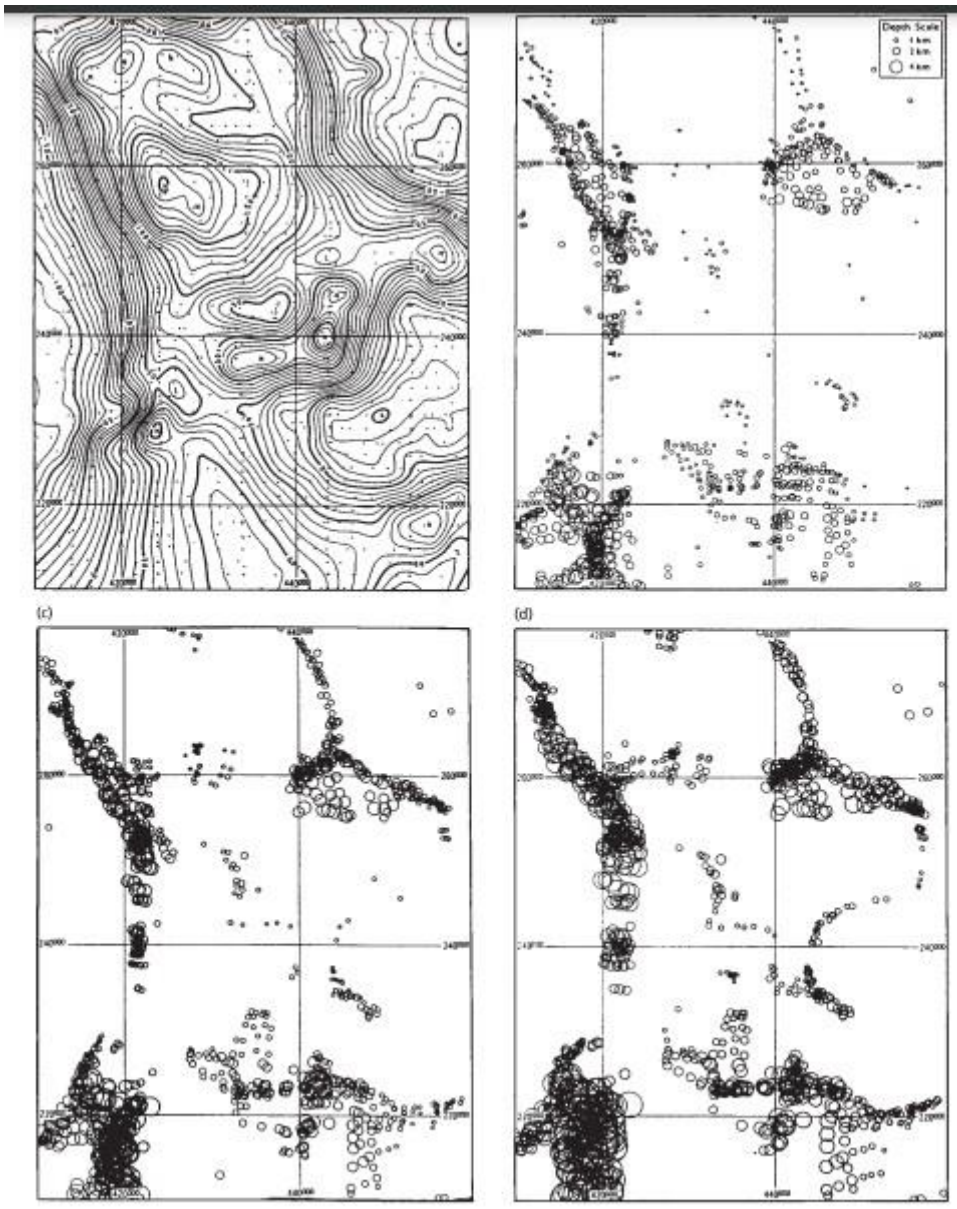

Fig. 7.17 (a) Observed aeromagnetic anomaly of a region in the English Midlands. Contour interval 10 nT. (b–d) Euler deconvolutions for structural indices 0.0 (b), 0.5 (c) and 1.0 (d). Source depth is indicated by the size of the circles. (e) Geological interpretation (*overleaf*). Grid squares are 10 km × 10 km in size. (After Reid *et al.* 1990.)

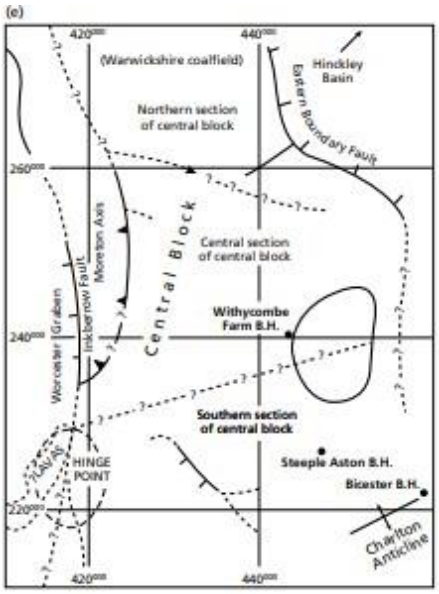

Fig. 7.17 *Continued*

respectively. The boundaries implied by the solutions have been used to construct the interpretation shown in Fig. 7.17(e).

7.10.3 Indirect interpretation

Indirect interpretation of magnetic anomalies is similar to gravity interpretation in that an attempt is made to match the observed anomaly with that calculated for a model by iterative adjustments to the model. Simple magnetic anomalies may be simulated by a single dipole. Such an approximation to the magnetization of a real geological body is often valid for highly magnetic ore bodies whose direction of magnetization tends to align with their long dimension (Fig. 7.18). In such cases the anomaly is calculated by summing the effects of both poles at the observation points, employing equations (7.10), (7.11) and (7.9). More complicated magnetic bodies, however, require a different approach.

The magnetic anomaly of most regularly-shaped bodies can be calculated by building up the bodies from a series of dipoles parallel to the magnetization direction

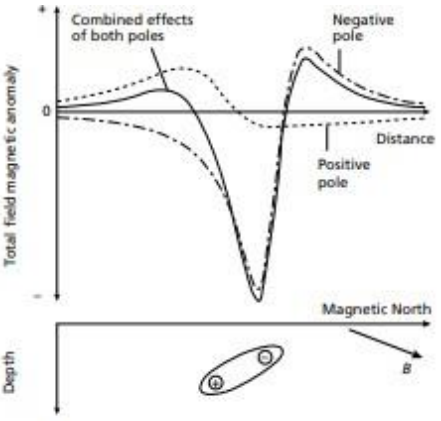

Fig. 7.18 The total field magnetic anomaly of an elongate body approximated by a dipole.

(Fig. 7.19). The poles of the magnets are negative on the surface of the body where the magnetization vector enters the body and positive where it leaves the body. Thus any uniformly-magnetized body can be represented by a set of magnetic poles distributed over its surface. Consider one of these elementary magnets of length l and cross-sectional area δA in a body with intensity of magnetization J and magnetic moment M. From equation (7.5)

$$M = J\delta A l \tag{7.15}$$

If the pole strength of the magnet is m, from equation (7.4) $m = M/l$, and substituting in equation (7.15)

$$m = J\delta A \tag{7.16}$$

If $\delta A'$ is the area of the end of the magnet and θ the angle between the magnetization vector and a direction normal to the end face

$$\delta A = \delta A' \cos\theta$$

Substituting in equation (7.16)

$$m = J\delta A' \cos\theta$$

thus

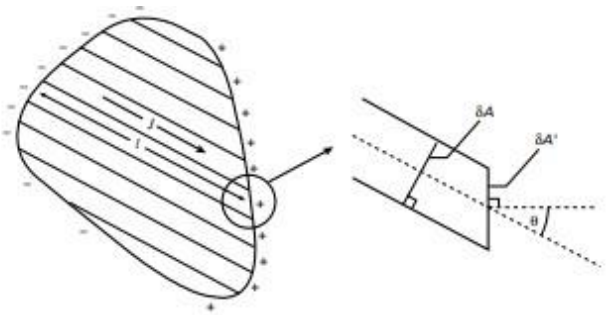

Fig. 7.19 The representation of the magnetic effects of an irregularly-shaped body in terms of a number of elements parallel to the magnetization direction. Inset shows in detail the end of one such element.

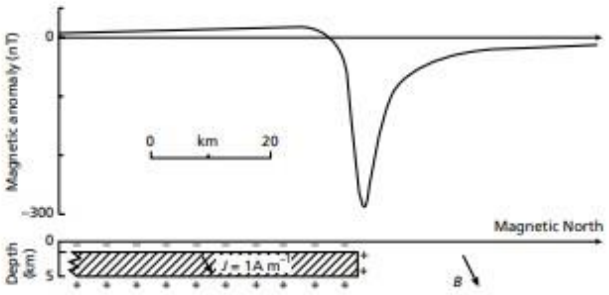

Fig. 7.20 The total field magnetic anomaly of a faulted sill.

pole strength per unit area = $J\cos\theta$ (7.17)

A consequence of the distribution of an equal number of positive and negative poles over the surface of a magnetic body is that an infinite horizontal layer produces no magnetic anomaly since the effects of the poles on the upper and lower surfaces are self-cancelling. Consequently, magnetic anomalies are not produced by continuous sills or lava flows. Where, however, the horizontal structure is truncated, the vertical edge will produce a magnetic anomaly (Fig. 7.20).

The magnetic anomaly of a body of regular shape is calculated by determining the pole distribution over the surface of the body using equation (7.17). Each small element of the surface is then considered and its vertical and horizontal component anomalies are calculated at each observation point using equations (7.10) and (7.11). The effects of all such elements are summed (integrated) to produce the vertical and horizontal anomalies for the whole body and the total field anomaly is calculated using equation (7.9). The integration can be performed analytically for bodies of regular shape, while irregularly-shaped bodies may be split into regular shapes and the integration performed numerically.

In two-dimensional modelling, an approach similar to gravity interpretation can be adopted (see Section 6.10.4) in which the cross-sectional form of the body is approximated by a polygonal outline. The anomaly of the polygon is then computed by adding or subtracting the anomalies of semi-infinite slabs with sloping edges corresponding to the sides of the polygon (Fig. 7.21). In the magnetic case, the horizontal ΔH, vertical ΔZ and total field ΔB anomalies (nT) of the slab shown in Fig. 7.21 are given by (Talwani *et al.* 1965)

$$\Delta Z = 200\sin\theta\,[J_x\{\sin\theta\log_e(r_2/r_1)+\phi\cos\theta\} + J_z\{\cos\theta\log_e(r_2/r_1)-\phi\sin\theta\}] \quad (7.18a)$$

$$\Delta H = 200\sin\theta\,[J_x\{\phi\sin\theta-\cos\theta\log_e(r_2/r_1)\} + J_z\{\phi\cos\theta+\sin\theta\log_e(r_2/r_1)\}]\sin\alpha \quad (7.18b)$$

$$\Delta B = \Delta Z\sin I + \Delta H\cos I \quad (7.18c)$$

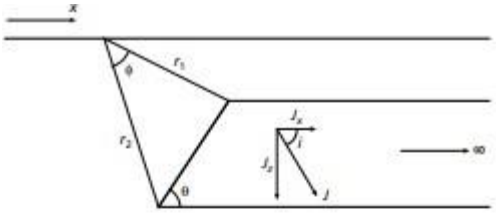

Fig. 7.21 Parameters used in defining the magnetic anomaly of a semi-infinite slab with a sloping edge.

where angles are expressed in radians, J_x ($= J\cos i$) and J_z ($= J\sin i$) are the horizontal and vertical components of the magnetization J, α is the horizontal angle between the direction of the profile and magnetic north, and I is the inclination of the geomagnetic field. Examples of this technique have been presented in Fig. 7.15. An important difference from gravity interpretation is the increased stringency with which the two-dimensional approximation should be applied. It can be shown that two-dimensional magnetic interpretation is much more sensitive to errors associated with variation along strike than is the case with gravity interpretation; the length–width ratio of a magnetic anomaly should be at least 10:1 for a two-dimensional approximation to be valid, in contrast to gravity interpretation where a 2:1 length–width ratio is sufficient to validate two-dimensional interpretation.

Three-dimensional modelling of magnetic anomalies is complex. Probably the most convenient methods are to approximate the causative body by a cluster of right rectangular prisms or by a series of horizontal slices of polygonal outline.

Because of the dipolar nature of magnetic anomalies, trial and error methods of indirect interpretation are difficult to perform manually since anomaly shape is not closely related to the geometry of the causative body. Consequently, the automatic methods of interpretation described in Section 6.10.3 are widely employed.

The continuation and filtering operations used in gravity interpretation and described in Section 6.11 are equally applicable to magnetic fields. A further processing operation that may be applied to magnetic anomalies is known as *reduction to the pole*, and involves the conversion of the anomalies into their equivalent form at the north magnetic pole (Baranov & Naudy 1964). This process usually simplifies the magnetic anomalies as the ambient field is then vertical and bodies with magnetizations which are solely induced produce anomalies that are axisymmetric. The existence of remanent magnetization, however, commonly prevents reduction to the pole from producing the desired simplification in the resultant pattern of magnetic anomalies.

7.11 Potential field transformations

The formulae for the gravitational potential caused by a point mass and the magnetic potential due to an isolated pole were presented in equations (6.3) and (7.3). A consequence of the similar laws of attraction governing gravitating and magnetic bodies is that these two equations have the variable of inverse distance ($1/r$) in common. Elimination of this term between the two formulae provides a relationship between the gravitational and magnetic potentials known as *Poisson's equation*. In reality the relationship is more complex than implied by equations (6.3) and (7.3) as isolated magnetic poles do not exist. However, the validity of the relationship between the two potential fields remains. Since gravity or magnetic fields can be determined by differentiation of the relevant potential in the required direction, Poisson's equation provides a method of transforming magnetic fields into gravitational fields and *vice versa* for bodies in which the ratio of intensity of magnetization to density remains constant. Such transformed fields are known as *pseudogravitational* and *pseudomagnetic* fields (Garland 1951).

One application of this technique is the transformation of magnetic anomalies into pseudogravity anomalies for the purposes of indirect interpretation, as the latter are significantly easier to interpret than their magnetic counterpart. The method is even more powerful when the pseudofield is compared with a corresponding measured field. For example, the comparison of gravity anomalies with the pseudogravity anomalies derived from magnetic anomalies over the same area can show whether the same geological bodies are the cause of the two types of anomaly. Performing the transformation for

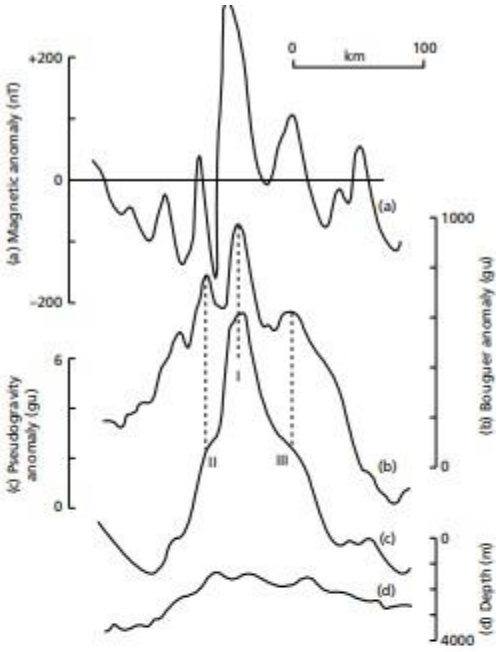

Fig. 7.22 (a) Observed magnetic anomalies over the Aves Ridge, eastern Caribbean. (b) Bouguer gravity anomalies with long-wavelength regional field removed. (c) Pseudo-gravity anomalies computed for induced magnetization and a density : magnetization ratio of unity. (d) Bathymetry.

different orientations of the magnetization vector provides an estimate of the true vector orientation since this will produce a pseudogravity field which most closely approximates the observed gravity field. The relative amplitudes of these two fields then provide a measure of the ratio of intensity of magnetization to density (Ates & Kearey 1995). These potential field transformations provide an elegant means of comparing gravity and magnetic anomalies over the same area and sometimes allow greater information to be derived about their causative bodies than would be possible if the techniques were treated in isolation. A computer program which performs pseudofield transformations is given in Gilbert and Galdeano (1985).

Figures 7.22(a) and (b) show magnetic and residual gravity anomaly profiles across the Aves Ridge, a submarine prominence in the eastern Caribbean which runs parallel to the island arc of the Lesser Antilles. The pseudogravity profile calculated from the magnetic profile assuming induced magnetization is presented in Fig. 7.22(c). It is readily apparent that the main pseudogravity peak correlates with peak I on the gravity profile and that peaks II and III correlate with much weaker features on the pseudofield profile. The data thus suggest that the density features responsible for the gravity maxima are also magnetic, with the causative body of the central peak having a significantly greater susceptibility than the flanking bodies.

Figure 7.23 shows how a variety of processing methods can be used on a synthetic magnetic anomaly map and Fig. 7.24 shows their application to real data.

7.12 Applications of magnetic surveying

Magnetic surveying is a rapid and cost-effective technique and represents one of the most widely-used geophysical methods in terms of line length surveyed (Paterson & Reeves 1985).

Magnetic surveys are used extensively in the search for metalliferous mineral deposits, a task accomplished rapidly and economically by airborne methods.

Magnetic surveys are capable of locating massive sulphide deposits (Fig. 7.25), especially when used in conjunction with electromagnetic methods (see Section 9.12). However, the principal target of magnetic surveying is iron ore. The ratio of magnetite to haematite must be high for the ore to produce significant anomalies, as haematite is commonly non-magnetic (see Section 7.2). Figure 7.26 shows total field magnetic anomalies from an airborne survey of the Northern Middleback Range, South Australia, in which it is seen that the haematitic ore bodies are not associated with the major anomalies. Figure 7.27 shows the results from an aeromagnetic survey of part of the Eyre Peninsula of South Australia which reveal the presence of a large anomaly elongated east–west. Subsequent ground traverses were performed over this anomaly using both magnetic and gravity methods (Fig. 7.28) and it was found that the magnetic and gravity profiles exhibit coincident highs. Subsequent drilling on these highs revealed the presence of a magnetite-bearing ore body at shallow depth with an iron content of about 30%.

Gunn (1998) has reported on the location of prospective areas for hydrocarbon deposits in Australia by aeromagnetic surveying, although it is probable that this application is only possible in quite specific environments.

In geotechnical and archaeological investigations, magnetic surveys may be used to delineate zones of faulting in bedrock and to locate buried metallic, man-made features such as pipelines, old mine workings and buildings. Figure 7.29 shows a total magnetic field contour map of the site of a proposed apartment block in Bristol, England. The area had been exploited for coal in the past and stability problems would arise from the presence of old shafts and buried workings (Clark 1986). Lined shafts of up to 2 m diameter were subsequently found beneath anomalies A and D, while other isolated anomalies such as B and C were known, or suspected, to be associated with buried metallic objects.

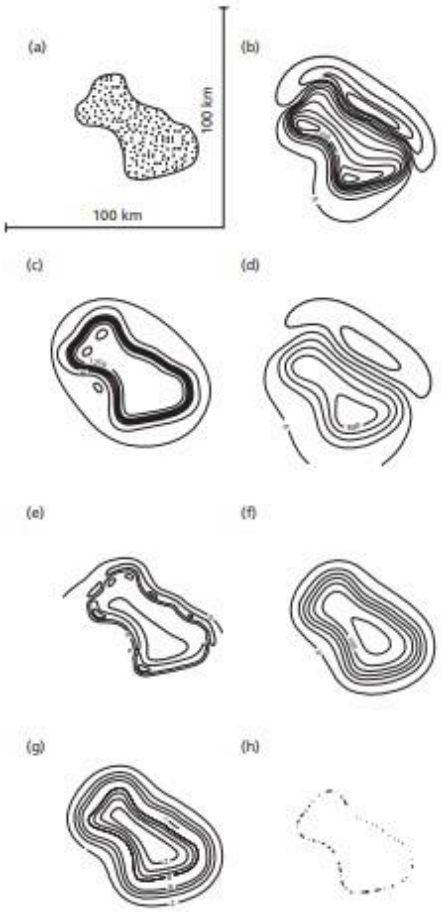

Fig. 7.23 The processing of aeromagnetic data. North direction is from bottom to top. (a) Source body with vertical sides, 2 km thick and a magnetization of 10 A m^{-1}, inclination 60° and declination 20°. (b) Total field magnetic anomaly of the body with induced magnetization measured on a horizontal surface 4 km above the body. Contour interval 250 nT. (c) Reduction to the pole of anomaly shown in (b). Contour interval 250 nT. (d) Anomaly shown in (b) upward continued 5 km above the measurement surface. Contour interval 200 nT. (e) Second vertical derivative of the anomaly shown in (b). Contour interval 50 nT km^{-2}. (f) Pseudogravity transform of anomaly shown in (b) assuming an intensity of magnetization of 1 A m^{-1} and a density contrast of 0.1 Mg m^{-3}. Contour interval 200 gu. (g) Magnitude of maximum horizontal gradient of the pseudogravity transform shown in (f). Contour interval 20 gu km^{-1}. (h) Locations of maxima of data shown in (g). Note correspondence with the actual edges of the source shown in (a). (Redrawn from Blakely & Connard 1989.)

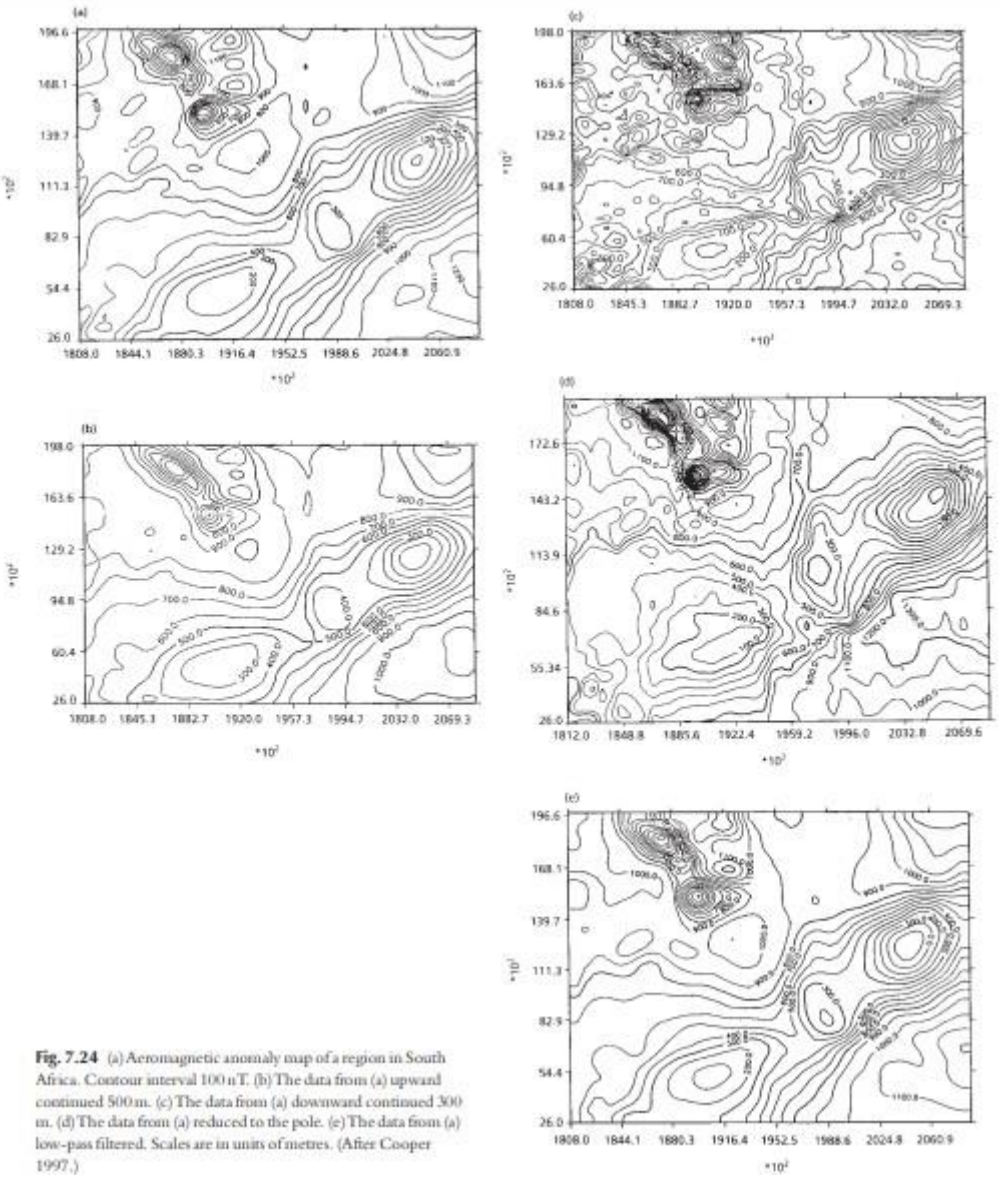

Fig. 7.24 (a) Aeromagnetic anomaly map of a region in South Africa. Contour interval 100 nT. (b) The data from (a) upward continued 500 m. (c) The data from (a) downward continued 300 m. (d) The data from (a) reduced to the pole. (e) The data from (a) low-pass filtered. Scales are in units of metres. (After Cooper 1997.)

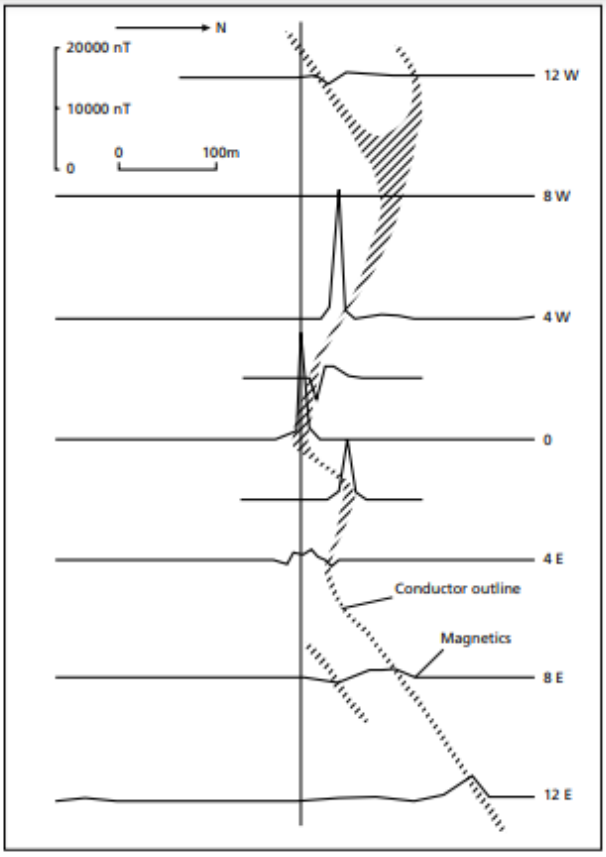

Fig. 7.25 Vertical field ground magnetic anomaly profiles over a massive sulphide ore body in Quebec, Canada. The shaded area represents the location of the ore body inferred from electromagnetic measurements. (After White 1966.)

In academic studies, magnetic surveys can be used in regional investigations of large-scale crustal features, although the sources of major magnetic anomalies tend to be restricted to rocks of basic or ultrabasic composition. Moreover, magnetic surveying is of limited use in the study of the deeper geology of the continental crust because the Curie isotherm for common ferrimagnetic minerals lies at a depth of about 20 km and the sources of major anomalies are consequently restricted to the upper part of the continental crust.

Although the contribution of magnetic surveying to knowledge of continental geology has been modest, magnetic surveying in oceanic areas has had a profound influence on the development of plate tectonic theory

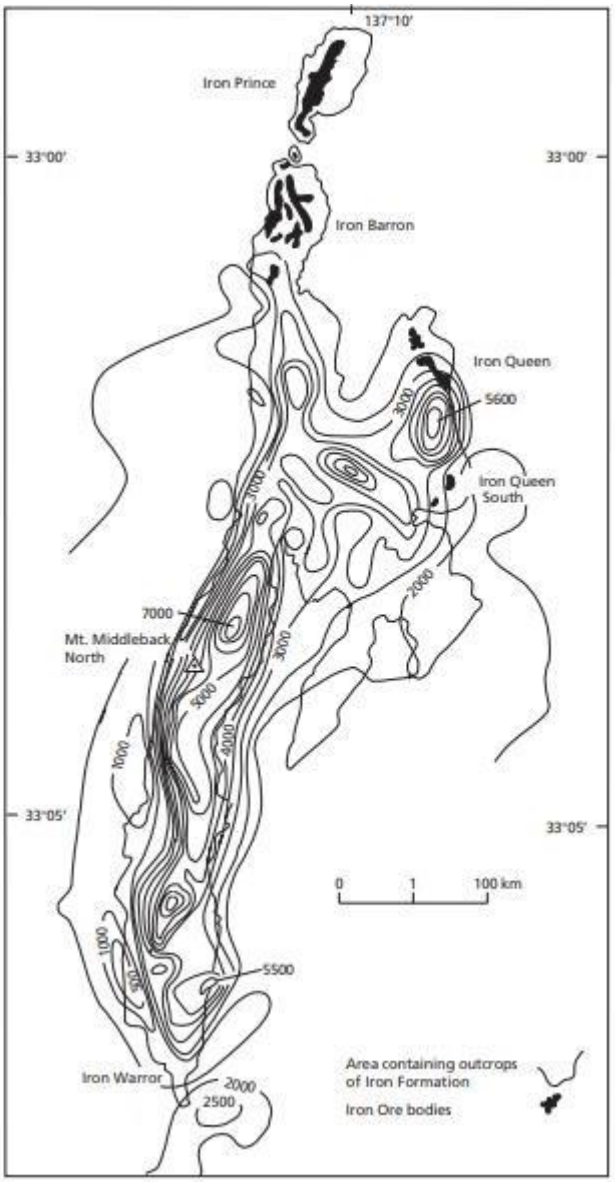

Fig. 7.26 Aeromagnetic anomalies over the Northern Middleback Range, South Australia. The iron ore bodies are of haematite composition. Contour interval 500 nT. (After Webb 1966.)

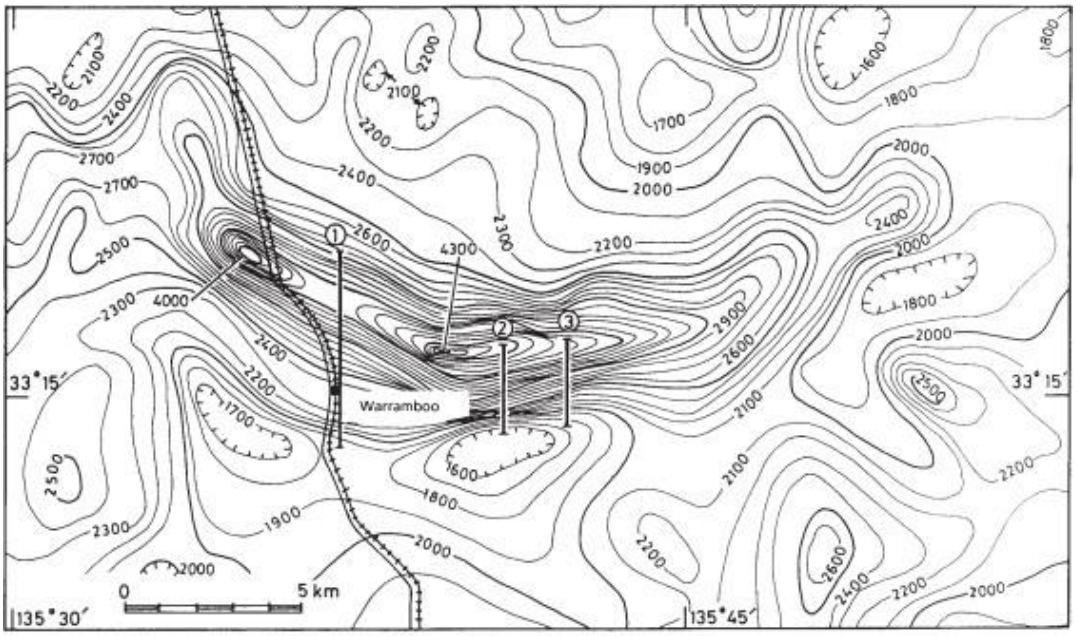

Fig. 7.27 High-level aeromagnetic anomalies over part of the Eyre Peninsula, South Australia. Contour interval 100 nT. (After Webb 1966.)

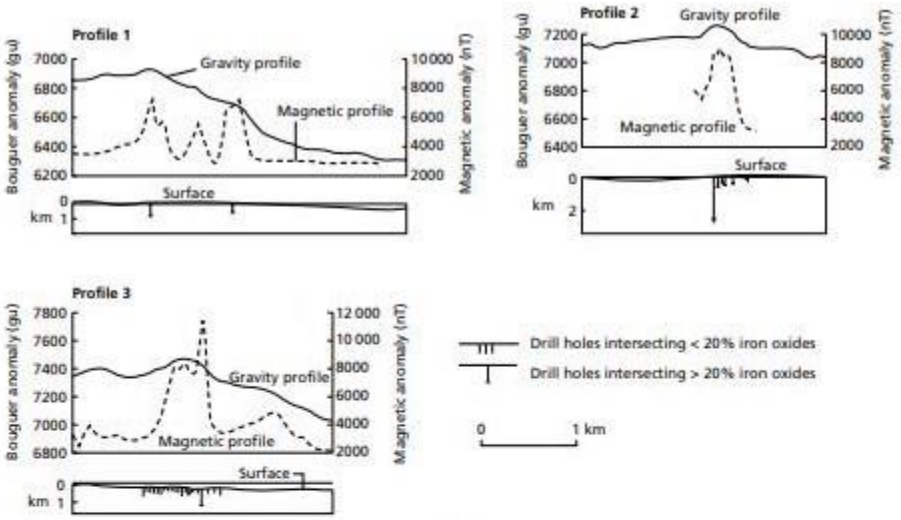

Fig. 7.28 Gravity and magnetic ground profiles over part of the Eyre Peninsula, South Australia, at the locations shown in Fig. 7.27 (After Webb 1966.)

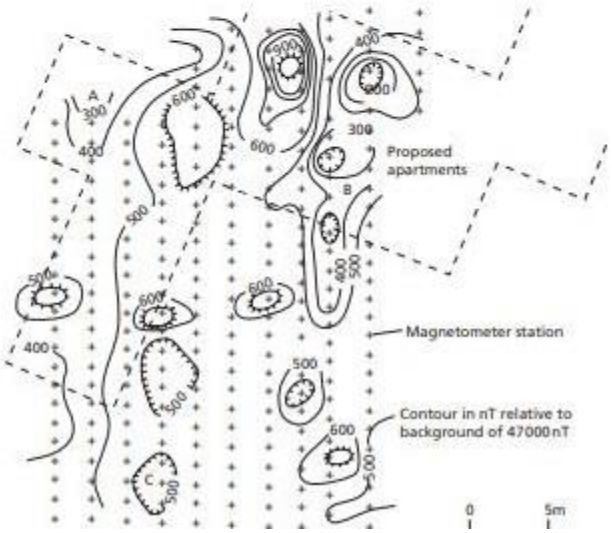

Fig. 7.29 Magnetic anomaly contour map of a site in Bristol, England. Contour interval 100 nT. (After Hooper & McDowell 1977.)

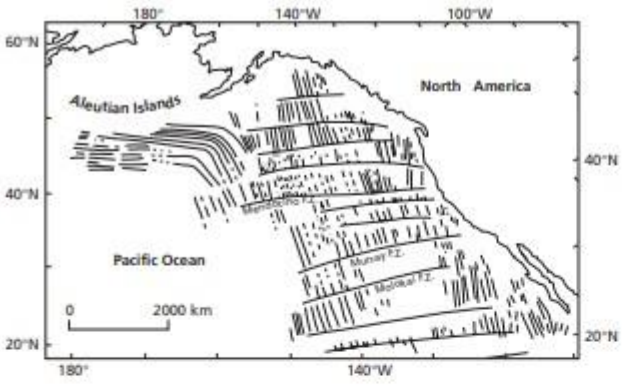

Fig. 7.30 Pattern of linear magnetic anomalies and major fracture zones in the northeast Pacific Ocean.

(Kearey & Vine 1996) and on views of the formation of oceanic lithosphere. Early magnetic surveying at sea showed that the oceanic crust is characterized by a pattern of linear magnetic anomalies (Fig. 7.30) attributable to strips of oceanic crust alternately magnetized in a normal and reverse direction (Mason & Raff 1961). The bilateral symmetry of these linear magnetic anomalies about oceanic ridges and rises (Vine & Matthews 1963) led directly to the theory of sea floor spreading and the establishment of a time scale for polarity transitions of the geomagnetic field (Heirtzler *et al.* 1968). Consequently, oceanic crust can be dated on the basis of the pattern of magnetic polarity transitions preserved in it.

Transform faults disrupt the pattern of linear magnetic anomalies (see Fig. 7.30) and their distribution can therefore be mapped magnetically. Since these faults lie along arcs of small circles to the prevailing pole of rotation at the time of transform fault movement, individual regimes of spreading during the evolution of an ocean basin can be identified by detailed magnetic surveying. Such studies have been carried out in all the major oceans and show the evolution of an ocean basin to be a complex process involving several discrete phases of spreading, each with a distinct pole of rotation.

Magnetic surveying is a very useful aid to geological mapping. Over extensive regions with a thick sedimentary cover, structural features may be revealed if magnetic horizons such as ferruginous sandstones and shales, tuffs and lava flows are present within the sedimentary sequence. In the absence of magnetic sediments, magnetic survey data can provide information on the nature and form of the crystalline basement. Both cases are applicable to petroleum exploration in the location of structural traps within sediments or features of basement topography which might influence the overlying sedimentary sequence. The magnetic method may also be used to assist a programme of reconnaissance geological mapping based on widely-spaced grid samples, since aeromagnetic anomalies can be employed to delineate geological boundaries between sampling points.

Problems

1. Discuss the advantages and disadvantages of aeromagnetic surveying.

2. How and why do the methods of reduction of gravity and magnetic data differ?

3. Compare and contrast the techniques of interpretation of gravity and magnetic anomalies.

4. Assuming the magnetic moment of the Earth is $8 \times 10^{22}\,\mathrm{A\,m^2}$, its radius 6370 km and that its magnetic field conforms to an axial dipole model, calculate the geomagnetic elements at 60°N and 75°S. Calculate also the total field magnetic gradients in $\mathrm{nT\,km^{-1}\,N}$ at these latitudes.

5. Using equations (7.18a,b,c), derive expressions for the horizontal, vertical and total field magnetic anomalies of a vertical dyke of infinite depth striking at an angle α to magnetic north.

Given that geomagnetic inclination I is related to latitude θ by $\tan I = 2 \tan \theta$, use these formulae to calculate the magnetic anomalies of east–west striking dykes of width 40 m, depth 20 m and intensity of magnetization $2\,\mathrm{A\,m^{-1}}$, at a latitude of 45°, in the following cases:

(a) In the northern hemisphere with induced magnetization.

(b) In the northern hemisphere with reversed magnetization.

(c) In the southern hemisphere with normal magnetization.

(d) In the southern hemisphere with reversed magnetization.

How would the anomalies change if the width and depth were increased to 400 m and 200 m, respectively?

6. (a) Calculate the vertical, horizontal and total field magnetic anomaly profiles across a dipole which strikes in the direction of the magnetic meridian and dips to the south at 30° with the negative pole at the northern end 5 m beneath the surface. The length of the dipole is 50 m and the strength of each pole is 300 A m. The local geomagnetic field dips to the north at 70°.

(b) What is the effect on the profiles if the dipole strikes 25°E of the magnetic meridian?

(c) If the anomalies calculated in (a) actually originate from a cylinder whose magnetic moment is the same as the dipole and whose diameter is 10 m, calculate the intensity of magnetization of the cylinder.

(d) Fig. 7.31 shows a total field magnetic anomaly profile across buried volcanic rocks to the south of Bristol, England. Does the profile constructed in (a) represent a reasonable simulation of this anomaly? If so, calculate the dimensions and intensity of magnetization of a possible magnetic source. What other information would be needed to provide a more detailed interpretation of the anomaly?

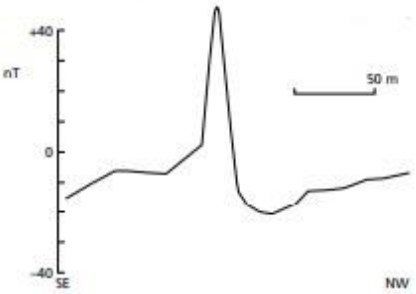

Fig. 7.31 Total field magnetic profile across buried volcanic rocks south of Bristol, England. (After Kearey & Allison 1980.)

References

Kearey, P. An Introduction to Geophysical Exploration. Department of Geology University of Leicester, Michael Brooks, 2002.